

DEPARTMENT OF THE INTERIOR

U.S. GEOLOGICAL SURVEY

**MINERALOGY OF URANIUM ORE FROM THE CROW BUTTE URANIUM DEPOSIT,  
OLIGOCENE CHADRON FORMATION, NORTHWESTERN NEBRASKA**

BY

P.L. Hansley<sup>1</sup>, S.P. Collings<sup>2</sup>, I.K. Brownfield<sup>1</sup>, and G.L. Skipp<sup>1</sup>

Open-File Report 89-225

This report is preliminary and has not been reviewed for conformity with U.S. Geological Survey editorial standards and stratigraphic nomenclature.

<sup>1</sup>U.S. Geological Survey, Denver, CO 80225

<sup>2</sup>Ferret Exploration Company of Nebraska, Inc., Denver, CO 80202

## ABSTRACT

The mineralogy of uranium ore from the Crow Butte uranium trend, a roll-type deposit in northwestern Nebraska, is dominated by micron-size coffinite crystals that are concentrated in the tuffaceous, pyritic matrix of basal sandstones in the Oligocene Chadron Formation. Uranium that is not in the coffinite structure is thought to be associated with submicron-size, X-ray amorphous minerals, adsorbed onto authigenic smectite, and/or contained in unaltered rhyolitic volcanic glass. Elements that are closely associated with uranium in the matrix are Ca, P, S, Fe, Si, Al, and V.

## INTRODUCTION

The Crow Butte uranium deposit, which was discovered in 1980 (Collings and Knode, 1984), is located in Dawes County, northwestern Nebraska (Fig. 1). Ore with an average grade in excess of 0.25 percent  $U_3O_8$  is currently being mined in an in-situ leaching operation by Ferret Exploration Company of Nebraska (Gjelsteen and Collings, 1988). Uranium occurs in the matrix of valley-fill sandstones in the basal sandstone member of the Chadron Formation of the Oligocene White River Group (Fig. 2). Uranium-bearing sandstones follow the trend of an early Oligocene braided stream valley that was cut into the underlying Upper Cretaceous Pierre Shale (Swinehart and others, 1985). In general, the basal ore-bearing sandstone is overlain by siltstones and claystones in the upper part of the Chadron, but in the vicinity of the Crow Butte deposit, it is directly overlain by a brick-red clay layer.

Apparent radiometric ages of 15.8 m.y. ( $^{206}Pb/^{238}U$ ) and 17.6 m.y. ( $^{207}Pb/^{235}U$ ) on ore (Gjelsteen, unpublished data, 1988) suggest that the uranium ore formed during the Miocene long after deposition of the Chadron in the early Oligocene (38-39 Ma). However, these ages are discordant suggesting that leakage of U daughter products has taken place. Petrographic data (e.g., grains surrounded by uraniferous matrix) suggest that the U mineralization occurred soon after deposition of the Chadron, while permeability of the sandstones remained high. Meteoric waters carrying dissolved uranyl species percolated through fluvial sandstones, and U precipitated upon encountering reductants, such as carbonaceous trash or sulfides. Gjelsteen and Collings (1988) proposed that ore-grade deposits formed along an oxidation/reduction front similar to Wyoming roll-front deposits (Harshman and Adams, 1981). The source of U is thought to have been rhyolitic volcanic ash (Fig. 3) that is abundant throughout the White River Group (Stanley and Benson, 1979). Zielinski (1983) analyzed ash from the White River Formation in Wyoming and found that it contained an average of 8 ppm U. He concluded that the ash was the probable source for U in underlying Eocene sandstone-hosted deposits there.

Framework minerals in sandstones of the Chadron Formation were probably derived from the Hartville uplift and Laramie Range in present-day northeastern Wyoming, but the airfall rhyolitic ash may have come from volcanoes far to the west in the Great Basin (Stanley and Benson, 1979). Swinehart and others (1985), however, suggested that the ash may have originated from volcanoes to the southwest in Colorado, because ash beds in the White River Group thin to the northeast.

This study characterizes the U mineralogy of the Crow Butte deposit, in part, to facilitate the in-situ leaching process. For this purpose, three composite ore samples (as much as 8-10 weight percent U) collected from three drillholes (depths of about 200 m) in the southern part of the known Crow

Butte uranium trend were analyzed by a variety of analytical techniques. Locations of the holes from which the core samples were taken are: T29N, R51W, section 1; T29N, R50W, section 29; and T31N, R51W, section 19.

## METHODS

Owing to the submicroscopic nature of the ore, a combination of analytical techniques was necessary to characterize the ore mineralogy. Even so, minerals may remain undetected, and some elements may reside in or be adsorbed onto the amorphous matrix and smectite rather than existing as discrete mineral phases. The most productive analytical techniques for mineral identification were X-ray diffraction and scanning electron microscopy (SEM). The energy dispersive system (EDS) of the SEM provided valuable data on elemental distribution in ore samples.

### Sample Preparation

Ore samples were ground in a ceramic mortar and pestle before most analyses were performed. After grinding, the sample was separated into various size fractions by sieving (see table 2 for sieve sizes).

### Alpha Counter

In order to determine which size fraction contained the most radioactive minerals, each fraction was counted with an alpha counter, which consists of a tube in a lead shield with an electronic scaler for readout.

### Heavy-Mineral Separation

Ore mineral grains in the 60-150 and 150-200  $\mu\text{m}$  fractions were concentrated by means of heavy-liquid (Bromoform) separation in funnels. For the smaller ( $<200 \mu\text{m}$ ) fraction centrifuging in Bromoform was necessary. A 40-ml centrifuge tube was filled about 40% full with Bromoform; a small amount of sample was then placed in the tube; the tube was agitated to place the sample in suspension in the Bromoform; the sample was placed in the centrifuge, which was run at 750-1000 rpm for 4 minutes. This process was then repeated. After centrifugation, the tube was placed in dry ice to freeze the bottom part of the tube which contained the heavy-mineral portion of the sample. The Bromoform containing the light minerals in suspension was then poured from the tube. After rinsing the tube with Bromoform to remove any residual light minerals, the tube was thawed and the heavy mineral fraction was rinsed with acetone onto a filter paper.

### X-Ray Diffraction

Various size fractions and heavy-mineral separates of ore-bearing sandstones were mounted in packed powder or collodion mounts and analyzed by X-ray diffraction with Cu radiation. In addition, hand-picked samples of ore were mounted on a gelatin fiber and analyzed in a Debye-Scherrer camera (diameter, 57.3 mm) with both Cu and Fe radiation. The camera was lined with Al-foil to reduce darkening of the X-ray film by alpha radiation from high-grade ore samples. Air-dried and glycolated oriented clay tiles were analyzed by X-ray diffraction to determine the clay mineralogy of ore-bearing sandstones.

## Scanning Electron Microscopy

The scanning electron microscope (SEM) was used to characterize ore textures and to determine the relations among ore and other authigenic minerals. Elemental distributions within the ore-bearing matrix were mapped with the SEM energy dispersive system (EDX). In order to study ore textures, small pieces of ore were mounted on Al stubs and coated with Au for maximum image resolution. Elemental distributions within ore were analyzed semi-quantitatively from polished grain mounts coated with C to allow the largest flux of secondary X-rays from the sample. Semi-quantitative elemental concentrations were obtained by analyzing the X-ray fluorescence spectra obtained from bombardment of an area of the sample with the electron beam. SEM micrographs (i.e., dot maps) of the X-ray fluorescence spectra of as many as 8 elements in a selected area of a polished section show the distributions of major elements relative to one another.

## Electron Microscopy

Aluminum-coated polished grain mounts of ore samples, which were handpicked from heavy-mineral separates (in order to concentrate U), were analyzed with the wavelength dispersive system of an electron microprobe to determine if there was a correlation between the occurrence of C and U. Quantitative analyses could not be performed because of the extremely fine grain size of the ore--ore minerals were commonly smaller than the diameter of the microprobe beam (about 1  $\mu\text{m}$ ).

## Thin Section Microscopy

Polished thin sections were examined with a petrographic microscope under direct reflected light in oil and under transmitted light to characterize textural relations between ore and other minerals. The heavy-mineral composition of sandstones was studied in grain mounts.

## DESCRIPTION OF ORE-BEARING SANDSTONES

Sandstones in the basal, ore-bearing part of the Chadron Formation are coarse-grained, tuffaceous arkosic litharenites; conglomerates containing pebbles and clay galls are present locally. The thickness of the basal sandstone in the ore trend averages 13 m (Gjelsteen and Collings, 1988). Polished sections of sandstone examined in transmitted light showed loosely packed, angular grains of quartz, plagioclase, K-feldspar, and rock fragments floating in a poorly sorted matrix of clay-size to fine-grained-sand size material. Feldspar grains are remarkably fresh and include abundant microcline and both twinned and untwinned plagioclase. Rock fragments are dominantly of granitic composition consisting of quartz and feldspars. Minor rock fragments include polycrystalline quartz (plutonic), chert, and metamorphic (micaceous) types.

Major nonopaque detrital heavy minerals are garnet, tourmaline, and zircon; minor types are staurolite, epidote, apatite, and biotite. Ilmenite and magnetite are the major opaque heavy minerals.

## DESCRIPTION OF ORE

X-ray fluorescence micrographs show that uranium is contained in the matrix of medium- to coarse-grained sandstones in the basal part of the Chadron Formation (Fig. 4). Uranium-bearing matrix also occurs between detrital muscovite plates (Fig. 5) and appears to have replaced margins of detrital albite (Fig. 6). When examined in polished section in oil, the U-bearing matrix has a low reflectivity and a gray-brown color; light-gray coffinite crystals less than 2 mm in length are associated with abundant authigenic pyrite (Fig. 7). Pyrite appears to be corroded where in contact with the U-bearing matrix (Fig. 8). Surface etching of pyrite (Fig. 9) and quartz (Fig. 10) was confirmed by SEM examination.

Even under the SEM, the U-bearing matrix exhibited uniform morphology (Fig. 11a), and SEM-EDS spectra consistently showed variable amounts of U, Si, P, V, Fe, Ca, and Al (Fig. 11b). Poorly developed micron-size coffinite crystals (Fig. 12) scattered throughout the matrix have a slightly higher reflectivity and have EDX spectra containing U, Si, P, Ca and less Fe and V than the surrounding matrix (Fig. 13). A few analyzed spots showed major U and trace amounts of other elements (Fig. 14).

SEM examination of orange-red (oxidized) ore revealed rosettes of tabular crystals (Fig. 15a) containing U and S (Fig. 15b), which may be zippeite, a hydrated uranyl sulfate, or a zippeite-like uranyl sulfate mineral (Fron del, 1958). Zippeite, however, cannot be positively identified without X-ray confirmation. Yellow (oxidized) ore is a mixture of ferric oxide and oxyhydroxides, possibly carnotite (where K and V accompany U), and pyrite.

An Al-coated ore sample examined with the electron microprobe showed no correlation between amounts of organic C and U. Organic C contents are relatively low (.02-.2 percent) in the Chadron (Gjelsteen and Collings, 1988); however, local accumulations of detrital plant material (as well as pyrite) probably served as reductants for U.

The chemical compositions of U-bearing minerals identified in the high-grade ore are listed on Table 1.

## RESULTS

### Alpha Counter

Uranium content of high-grade ore is inversely correlated with grain size with the result being that the highest concentrations of U reside in the clay fraction (64,000 cps) (Table 2).

### X-ray Diffraction

Minerals identified in X-ray diffractograms of the <200 mesh (<.074 mm) fraction were, in order of decreasing abundance: quartz, plagioclase, K-feldspar, coffinite, pyrite, marcasite, calcite, illite/smectite, and tyuyamunite. Other minerals that may be present in amounts too small to be detected or that have spectral interferences with more common minerals, include carnotite, metatyuyamunite, and uraninite. The high background on all X-ray diffractograms is due to the presence of abundant (amorphous) volcanic glass. The centrifuged heavy-mineral portion of the <200 mesh fraction contained, in order of decreasing abundance: quartz, coffinite, K-feldspar, plagioclase, uraninite(?), garnet, pyrite, magnetite, calcite, marcasite, ilmenite, tyuyamunite(?), and illite (Table 3).

X-ray films of high-graded grains of ore showed only dominant reflections of major mineral species due to fogging of the film by alpha radiation (despite the Al-foil lining in the camera): quartz and pyrite were accompanied by weak coffinite, feldspar, and uraninite(?) reflections (Table 4).

In order to further concentrate ore minerals for identification, heavy-mineral separations were made using the 150-60 mesh (100-250  $\mu\text{m}$ ) fraction. The resultant heavy-mineral separates analyzed by X-ray diffraction included the following minerals: quartz, garnet, marcasite, pyrite, coffinite, plagioclase, and K-feldspar. Minor uraninite, tyuyamunite, and metatyuyamunite may also be present. Marcasite (Fig. 16) was nearly as abundant as pyrite in many samples. Garnet is consistently the most common mineral in the heavy-mineral separates. Large amounts of quartz and feldspar in heavy-mineral separates resulted from adherence of uraniferous matrix to framework grains making them heavier and pulling them down during the separation process.

X-ray diffractograms of the  $<2 \mu\text{m}$  fraction showed small amounts of smectite that was 90 percent expandable.

## DISCUSSION

Coffinite, which is the major U-bearing mineral in the Crow Butte deposit, is intimately associated with pyrite. Widespread corrosion textures of pyrite suggest that oxidation of pyrite was instrumental in the reduction and precipitation of U. Gjelsteen and Collings (1988) proposed that oxidizing ground water in the Chadron Formation picked up dissolved sulfur, which had diffused upward from the underlying Pierre Shale. Subsequent bacterially mediated sulfate reduction of detrital organic matter in the Chadron produced  $\text{H}_2\text{S}$  that combined with Fe to form pyrite. Uranium, which was carried in solution by meteoric waters as the uranyl ion, was adsorbed and then reduced to the uranous ion upon encountering concentrations of pyrite and organic matter. High silica activity due to dissolution of the rhyolitic ash favored formation of coffinite over uraninite (Hemingway, 1982) in most parts of the sandstone. The association of Ca and P with U and Si in the matrix suggests that as Ca (2+) substituted for U (4+), P (5+) proxied for Si (4+) effectively maintaining the charge balance in the coffinite structure. Coupled substitution of Ca and Y for U and P for Si was noted by Hansley and Fitzpatrick (1989) in coffinite from the Grants uranium region, New Mexico. Rare earth elements (REE's) were not identified in the spectra of Crow Butte ore, although small amounts of heavy REE's may be present, as suggested by a broad hump in the spectral region of Al on many EDX spectra.

Vanadium and Fe commonly appear in SEM-EDX spectra with U and Si, but neither element should proxy in the coffinite structure because of incompatible ionic radii ( $\text{U}^{4+}$ , .97;  $\text{V}^{3+}$ , .74; and  $\text{Fe}^{2+}$ , .76; Sargent-Welch, 1968). Iron is probably contained in smectite, iron disulfides, iron oxides, and iron oxyhydroxides. The presence of V, however, is somewhat of a mystery, because no V minerals with the exception of tyuyamunite and metatyuyamunite(?) were detected on X-ray diffractograms. Matrix containing the most V appeared to be amorphous, even under highest SEM magnification; thus, some V may still be bound in amorphous glassy material. Some V could also be associated with organic matter. Vanadium may have been derived from dissolution of the rhyolitic ash, because ashes examined from localities worldwide are enriched in V over U by a factor of 10-100x (Smith and others, 1982). In sandstone-hosted uranium deposits of the Grants uranium region, alteration of detrital

Fe-Ti oxides is thought to have been a source of V (Reynolds and others, 1986). However, all Fe-Ti oxides observed in heavy-mineral separates of Crow Butte ore were unaltered (Fig. 17).

In general, marcasite is indicative of formation at a lower pH than pyrite (Goldhaber and Kaplan, 1974). However, the paragenesis of marcasite was not determined.

The sulfates, gypsum and zippeite(?), noted during SEM examination of the ore may be products of recent oxidation of sulfides and coffinite, for ground water in the Chadron is presently a Na-SO<sub>4</sub>-HCO<sub>3</sub>-Cl water (Gjelsteen and Collings, 1988). Alternatively, oxidation of ore may have occurred between the time (about 3 years) between the collection of cores and petrographic examination.

The smectite is thought to have been derived from alteration of volcanic ash during early diagenesis (Stanley and Benson, 1979). The possibility that some of the smectite is detrital cannot be ruled out; however, the high expandability of the smectite and the association of the smectite with volcanic ash indicate an authigenic rather than a detrital origin. Major oxidation of ore may have been prevented by the lowering of sandstone permeability by smectite-filled pores.

## CONCLUSIONS

The Crow Butte deposit has been interpreted to be a roll-front deposit on the basis of paleo-ground water hydrology, oxidation/reduction fronts, and morphology of the deposit (Gjelsteen and Collings, 1988). Petrographic data (e.g., U-bearing matrix at grain contacts) indicate that U mineralization occurred before lithification of the sandstone. Dissolution of abundant rhyolitic volcanic ash produced U- and Si-rich ground waters that were channeled through permeable sandstones at the base of the Chadron by relatively impermeable overlying and underlying beds. The precipitation of early authigenic pyrite created a reducing environment favorable for precipitation and accumulation of U in the basal sandstone. The U has remained in a reduced state, as evidenced by the fact that the unoxidized minerals, coffinite and uraninite, comprise the bulk of the ore. At least some U and V remain bound to amorphous volcanic material and/or smectite rather than existing as discrete mineral phases.

## REFERENCES CITED

- Collings, S.P., and Knode, R.H., 1984, Geology and discovery of the Crow Butte uranium deposit, Dawes County, Nebraska: Practical Hydromet '83: 7th Annual Symposium on Uranium and Precious Metals, American Institute of Metallurgical Engineers, p. 5-14.
- Fron del, Clifford, 1958, Systematic mineralogy of uranium and thorium: U.S. Geological Survey Bulletin 1064, 400 p.
- Gjelsteen, T.W., and Collings, S.P., 1988, Relationship between groundwater flow and uranium mineralization in the Chadron Formation, northwest Nebraska: Wyoming Geological Association Guidebook, 39th Field Conference, p. 271-284.
- Goldhaber, M.B., and Kaplan, I.R., 1974, The sulfur cycle in Goldberg, E.D., ed., The Sea: Marine Chemistry, Vol. 5, Wiley, New York, p. 569-655.
- Hansley, P.L., and Fitzpatrick, Joan, 1989, Compositional and crystallographic data on REE-bearing coffinite from the Grants uranium region, northwestern New Mexico: American Mineralogist, v. 74, p. 263-270.

- Harshman, E.N., and Adams, S.S., 1981, Geology and recognition criteria for roll-type uranium deposits in continental sandstones: U.S. Department of Energy, GJBX-1(81), 185 p.
- Hemingway, B.S., 1982, Thermodynamic properties of selected uranium compounds and aqueous species at 298.15 degrees K and 1 bar and at higher temperatures--Preliminary models for the origin of coffinite deposits: U.S. Geological Survey Open-file Report 82-619, 60 p.
- Reynolds, R.L., Fishman, N.S., Scott, J.H., and Hudson, M.R., 1986, Iron-titanium oxide minerals and magnetic susceptibility anomalies in the Mariano Lake-Lake Valley cores--constraints on conditions of uranium mineralization in the Morrison Formation, San Juan basin, New Mexico, in Turner-Peterson, C.E., Santos, E.S., and Fishman, N.S., eds., A basin analysis case study--The Morrison Formation, Grants uranium region, New Mexico: American Association of Petroleum Geologists Studies in Geology No. 22, p. 303-314.
- Sargent-Welch Scientific Company, 1968, Table of Periodic Properties of the Elements, 1 p.
- Smith, D.K., Jr., 1984, Uranium mineralogy, in De Vivo, B., Ippolito, F., Capaldi, G., and Simpson, P.R., eds.: Uranium geochemistry, mineralogy, geology, exploration, and resources, London, The Institution of Mining and Metallurgy, p. 43-379.
- Smith, D.B., Zielinski, R.A., and Rose, W.I., Jr., 1982, Leachability of uranium and other elements from freshly erupted volcanic ash: Journal of volcanology and geothermal research, v. 13, p. 1-30.
- Stanley, K.O., and Benson, L.V., 1979, Early diagenesis of High Plains vitric and arkosic sandstones, Wyoming and Nebraska: Society of Economic Paleontologists and Mineralogists Special Publication No. 26, p. 401-423.
- Swinehart, J.B., Souders, V.L., DeGraw, H.M., and Diffendal, R.F., Jr., 1985, Cenozoic paleogeography of western Nebraska, in Flores, R.M., and Kaplan, S.S., eds., Cenozoic paleogeography of the west-central United States: Rocky Mountain Section, Society of Economic Paleontologists and Mineralogists, p. 187-206.
- Zielinski, R.A., 1983, Tuffaceous sediments as source rocks for uranium: a case study of the White River Formation, Wyoming: Journal of Geochemical Exploration, v. 18, p. 285-306.

Table 1.--Chemical compositions (Smith, 1984) of U-bearing minerals that may be present in high-grade ore.

Mineral	Composition
Coffinite	$U(SiO_4)_{1-x}(OH)_{4x}$
Uraninite	$UO_2$
Tyuyamunite	$Ca(UO_2)_2(VO_4)_2 \cdot 5-8H_2O$
Metatyuyamunite	$Ca(UO_2)_2(VO_4)_2 \cdot 3-5H_2O$
Carnotite	$K_2(UO_2)_2(VO_4)_2 \cdot 3H_2O$
Zippeite	$K_4(UO_2)_6(SO_4)_3(OH)_{10} \cdot 16H_2O$

Table 2.--Alpha counts in various size fractions (mesh) of medium- and high-grade Crowe Butte uranium ore (Average background, 100 cps)

Size Fraction	Medium grade (cps)	High grade (cps)
Clay	4539	64472
<200	2626	50169
>200<150	1698	28515
>150<60	1524	22845
>60	812	9186

Table 3.--Minerals detected in X-ray diffractogram of centrifuged heavy-mineral fraction (S.G.>2.87) of high-grade ore (Cu radiation, Ni filter).

d(A) <sup>1</sup>	I <sup>2</sup>	hkl	Mineral
3.34	>100	101	Quartz
3.48	44.5	200	Coffinite
3.25	39.1	040,202	K-feldspar
3.19	39.0	040	Plagioclase
3.16	29.0	111	Uraninite(?)
2.58	28.9	420	Garnet
1.64	28.0	311	Pyrite
2.53	23.5	311	Magnetite
3.04	20.1	104	Calcite
2.71	15.0	020,101	Marcasite <sup>3</sup>
10.2	11.0	020	Tyuyamunite(?)
1.72	15.0	116	Ilmenite
10.0	10.7	001	Illite

<sup>1</sup> Chart units.

<sup>2</sup> Reflection of 100% intensity chosen for each mineral species; abundances are strictly relative.

<sup>3</sup> Pyrite (200) subtracted from marcasite reflections.

Table 4.--X-ray powder diffraction data for high-grade ore [Fe radiation, Mn filter; 5 hour exposure in Al-foil-lined 57.3 mm camera].

<u>d(A)</u>	<u>I</u> <sup>1</sup>	<u>hkl</u>	<u>Mineral</u>
4.24	S	100	Quartz
3.85	VW	111	Feldspar(?)
3.80	W	111	Feldspar(?)
3.55	VW	130,131	Feldspar(?)
3.48	VW	200	Coffinite
3.39	M	101	Quartz
3.17	VW	111,040	Uraninite, feldspar
2.74	VS	200(020,101)	Pyrite (marcasite)
2.45	S	210	Pyrite
2.35	VW	120(?)	Marcasite(?)
2.24	M	211	Pyrite
1.93	M	220	Pyrite
1.77	W	312,211	Coffinite, marcasite
1.65	VS	311	Pyrite
1.62	VW	113	Uraninite(?)
1.51	VW	230	Pyrite
1.46	VW	321	Pyrite

<sup>1</sup> VS, very strong; S, strong; M, moderate; W, weak; VW, very weak.

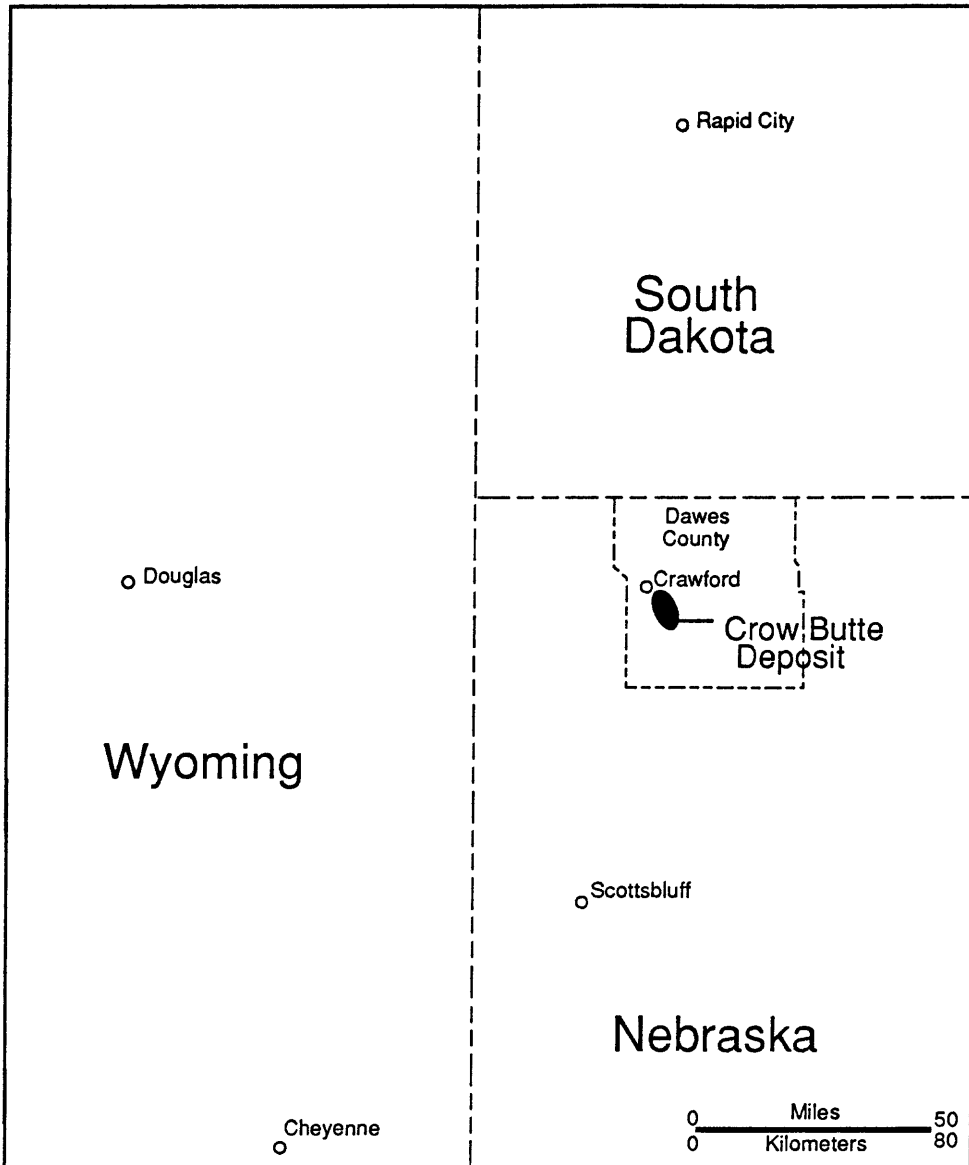


Figure 1.--Index map showing location of the Crow Butte uranium deposit.

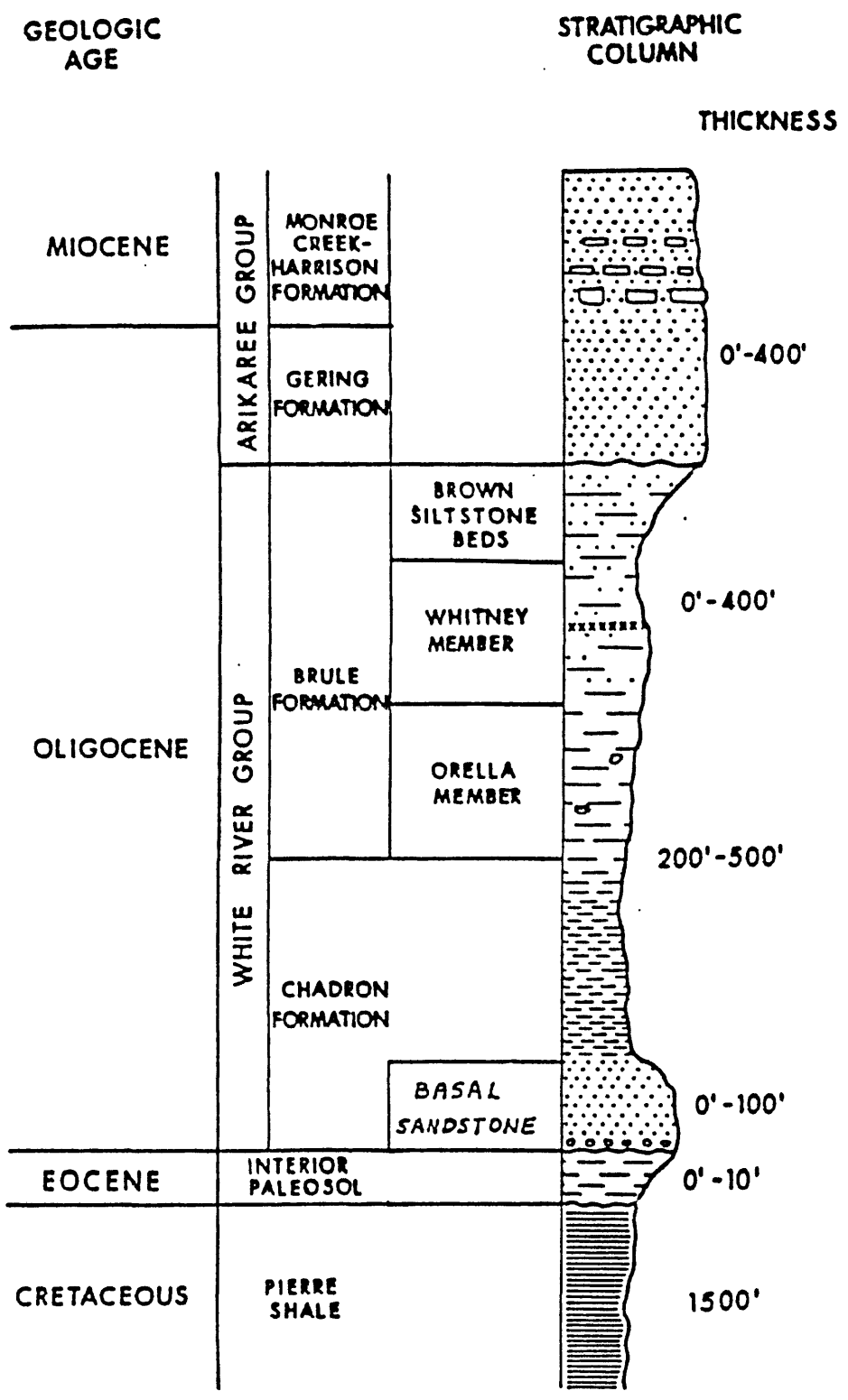


Figure 2.--Stratigraphy of the White River Group in the vicinity of the Crow Butte deposit, northwestern Nebraska (based on Swinehart and others, 1985)

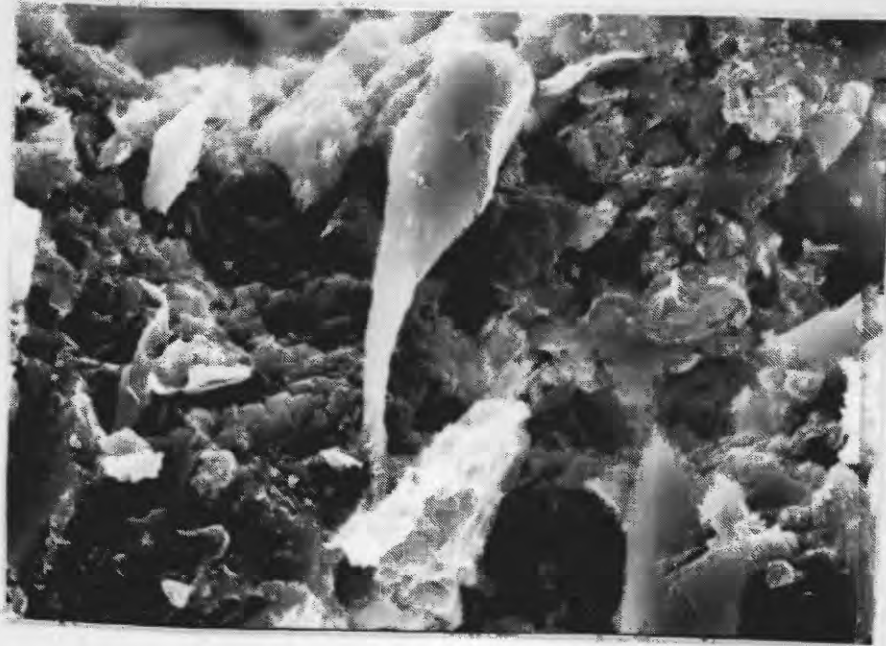
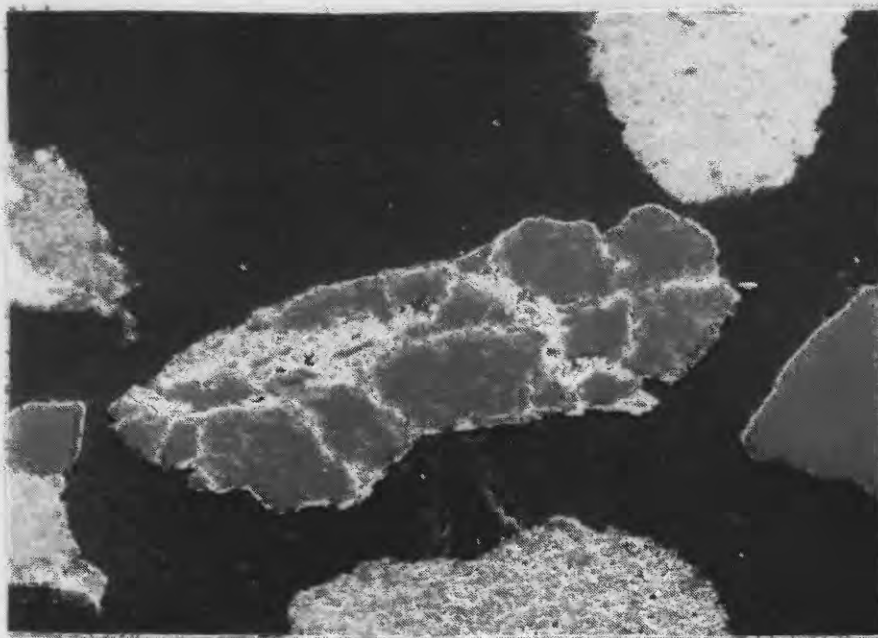
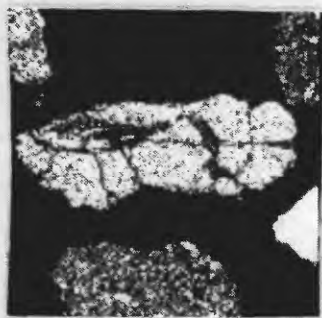


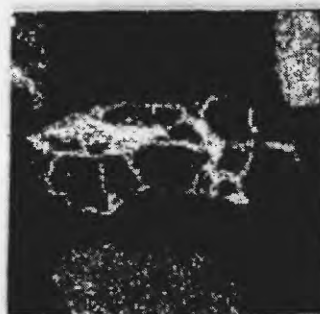
Figure 3.--Scanning electron micrograph (SEM) of a volcanic shard in sandstone of the Chadron Formation. Length of field of view is 30  $\mu\text{m}$ .



A



Si



U

B

Figure 4.--(A) SEM micrograph of typical Crow Butte ore: sandstone with uraniferous, tuffaceous matrix. Length of field of view is 0.5 mm.

(B) X-ray fluorescence micrographs of U and Si (as concentrations of white dots) in 4A showing that U is concentrated in the matrix; Si distribution represents quartz grains. Length of field of view is 1.2 mm. Counting time, 40 minutes.

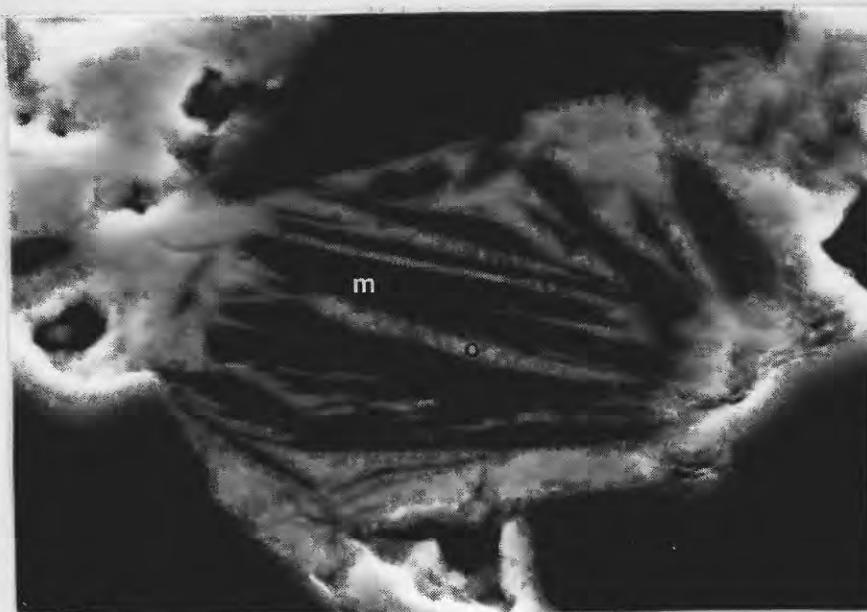


Figure 5.--SEM micrograph of uraniumiferous matrix (o) between muscovite plates (m) in high-grade ore. Length of field of view is 20  $\mu\text{m}$ .

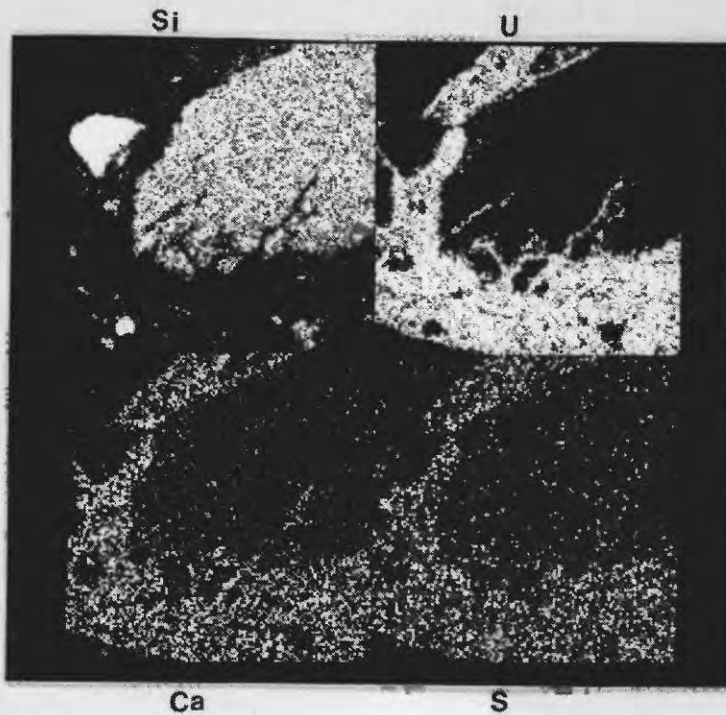


Figure 6.--X-ray fluorescence micrograph of uraniferous matrix that has apparently replaced the margins of a detrital albite grain. White dots represent the distribution of U, Si, Ca, and S. Length of field of view is 0.2 mm. Counting time, 40 minutes.

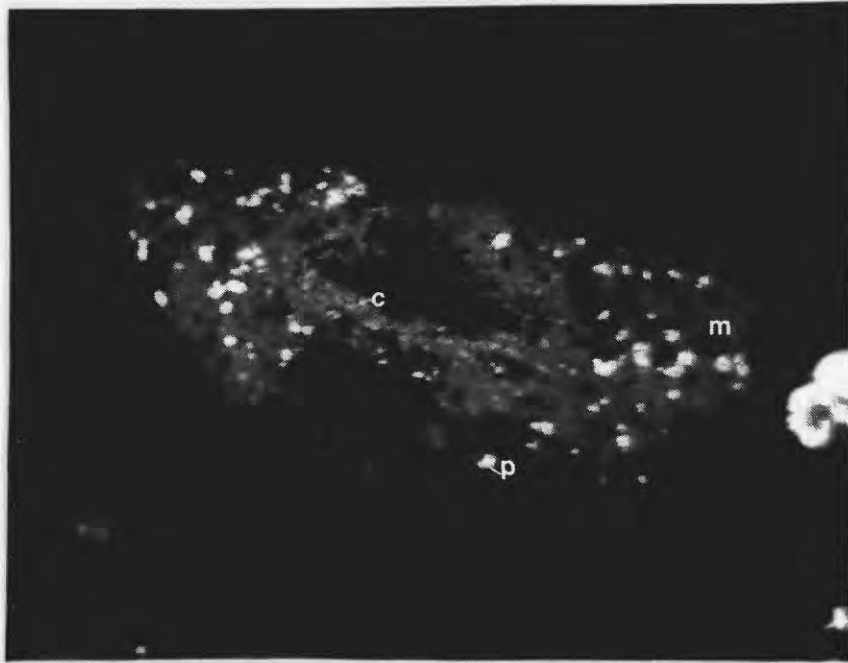


Figure 7.-- Photomicrograph of uranium-bearing, gray-brown matrix (m) with micron-size, light-gray coffinite crystals (c) and yellowish white pyrite (p). Length of field of view is 100  $\mu\text{m}$ . Direct reflected light; oil immersion.

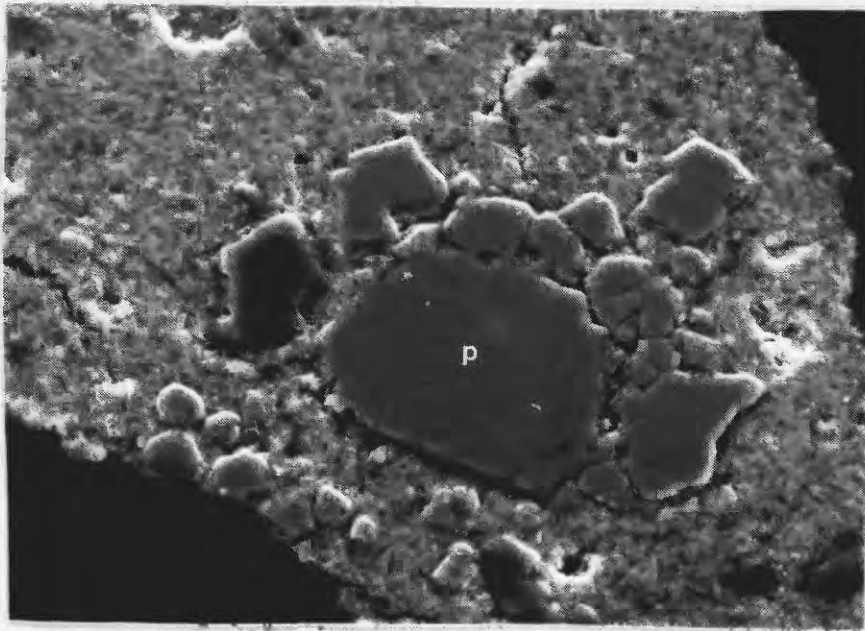


Figure 8.--SEM micrograph of corroded pyrite (p) in uranium-bearing matrix. Direct reflected light; oil immersion. Length of field of view is 70  $\mu\text{m}$ .

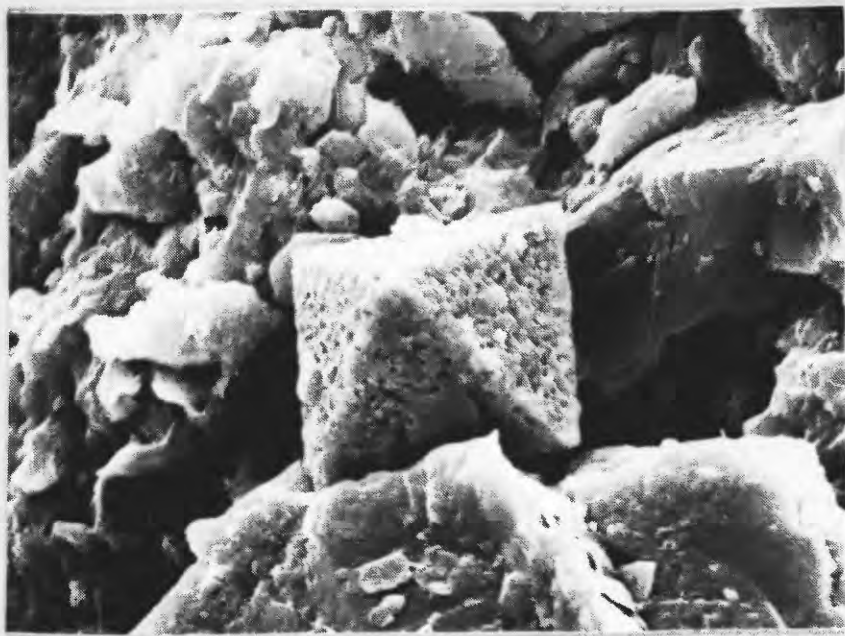


Figure 9.--SEM micrograph of etched euhedral pyrite. Length of field of view is 28  $\mu\text{m}$ .

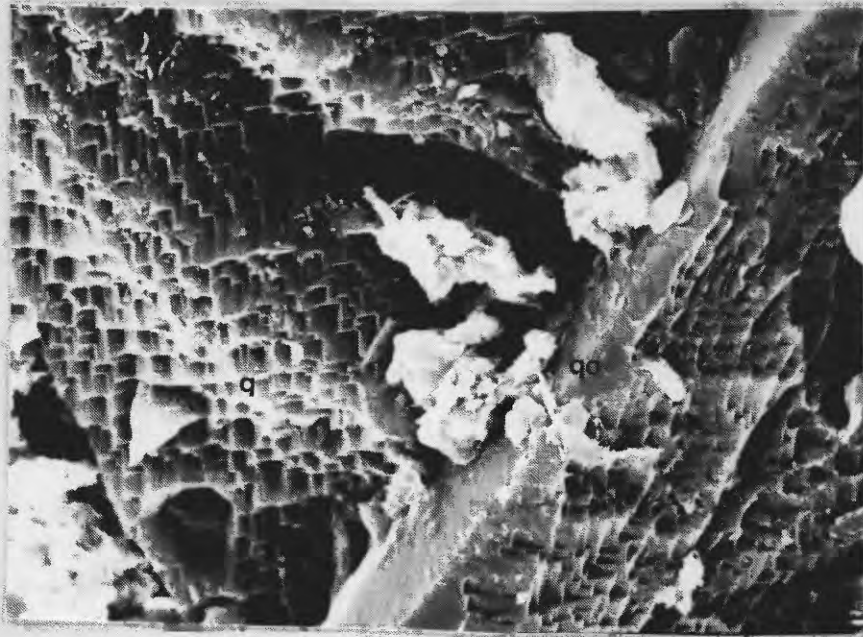
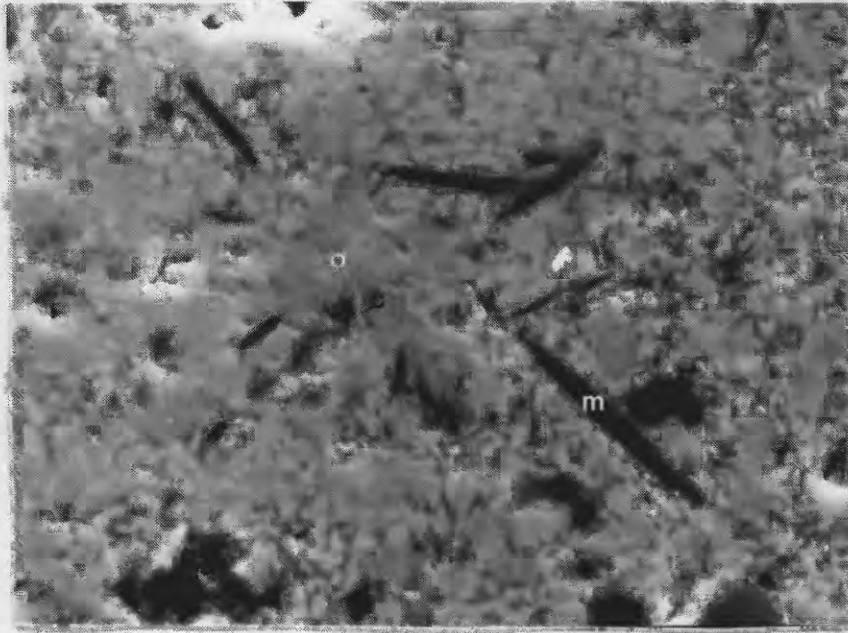
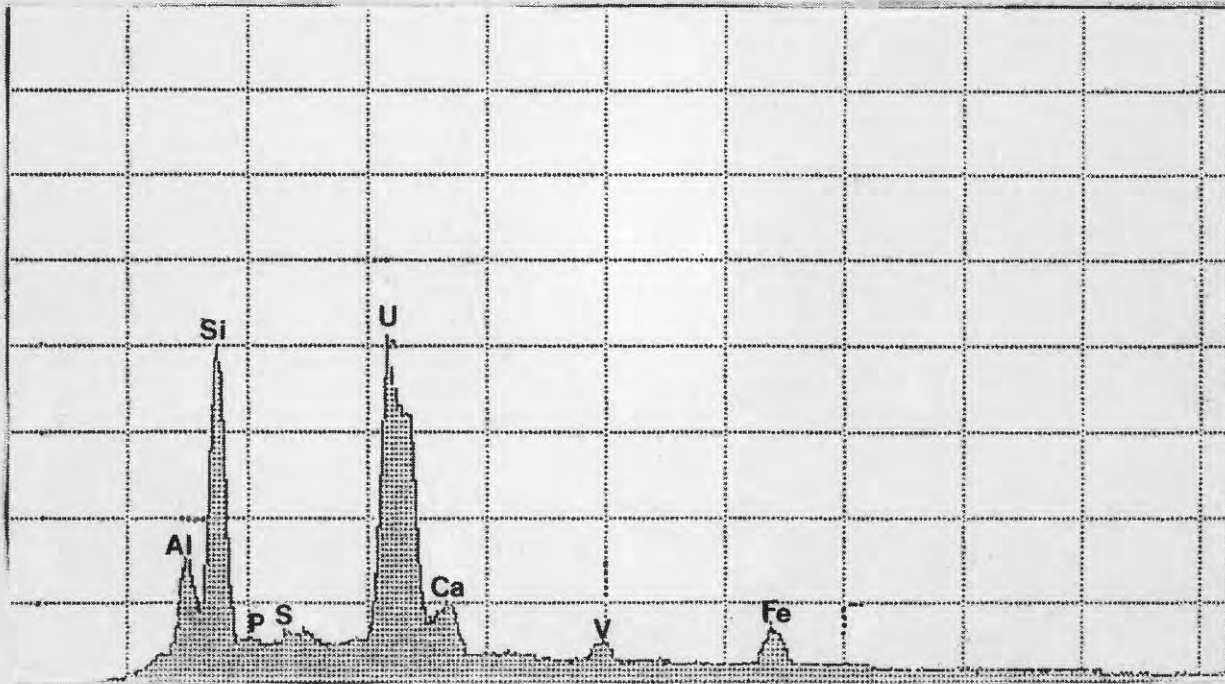


Figure 10.--SEM micrograph of etched quartz grain (q) and quartz overgrowth (qo). Length of field of view is 24  $\mu\text{m}$ .



A



B

Figure 11.--(A) SEM micrograph of polished section shows apparently amorphous character of ore (o); however, note micron-size coffinite laths (c) that are lighter-colored than matrix. Larger thin black plates are mica (m). Length of field of view is 30  $\mu\text{m}$ .  
 (B) SEM-EDX spectra of uraniferous matrix in 4A. Counting time, 30 seconds.

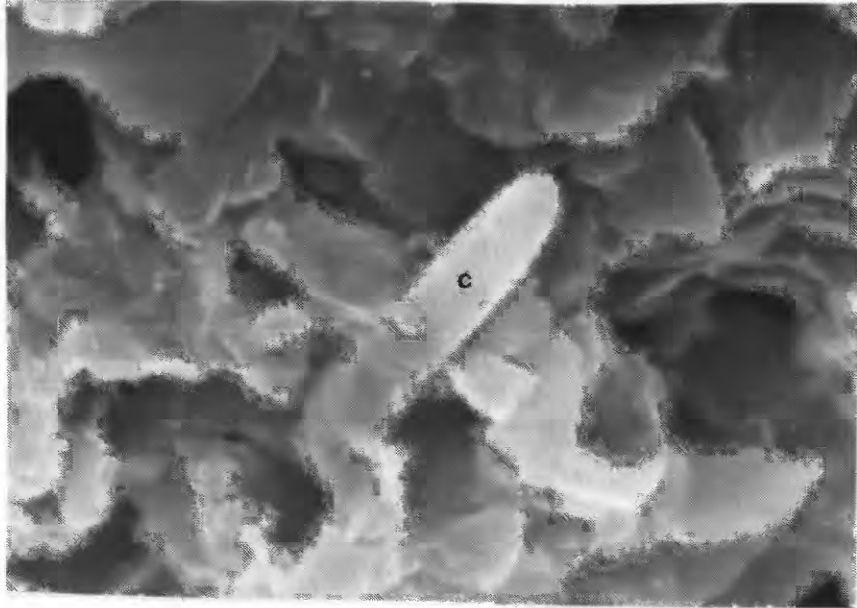


Figure 12.--SEM micrograph of typical poorly-formed, micron-size coffinite crystal (c) in uranium-bearing matrix. Length of field of view is 6  $\mu\text{m}$ .

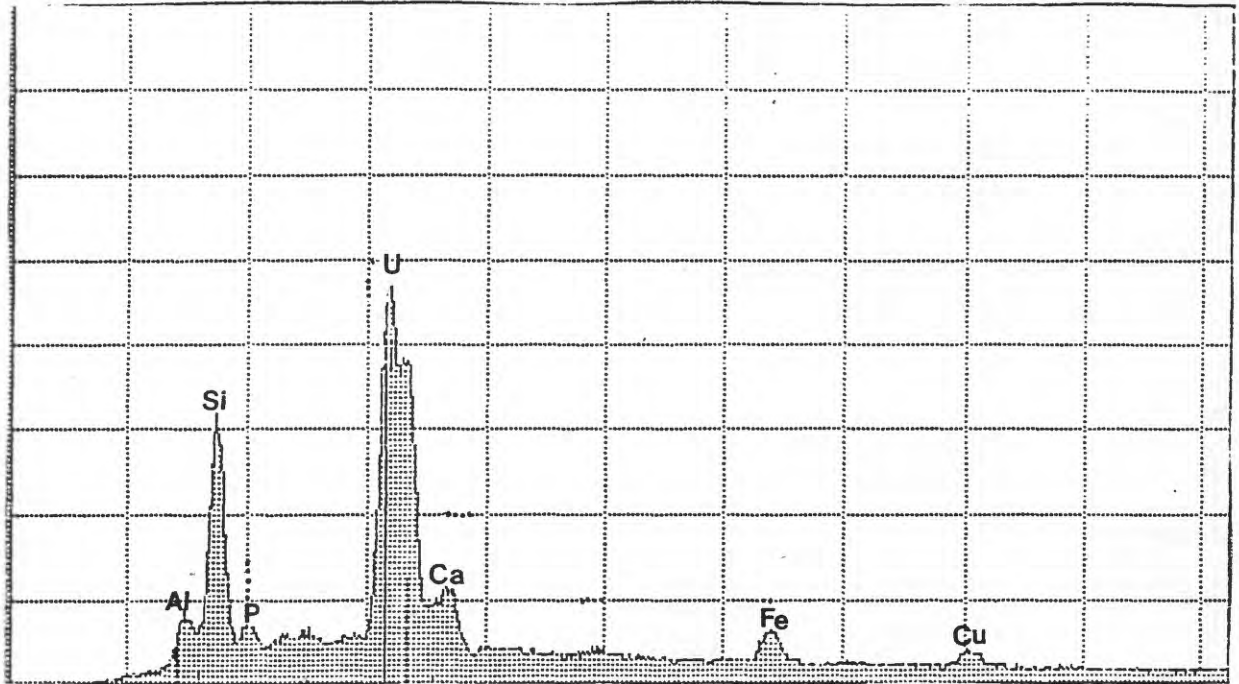


Figure 13.--SEM-EDX spectra of brighter areas of U-bearing matrix in polished section inferred to contain higher concentrations of coffinite.

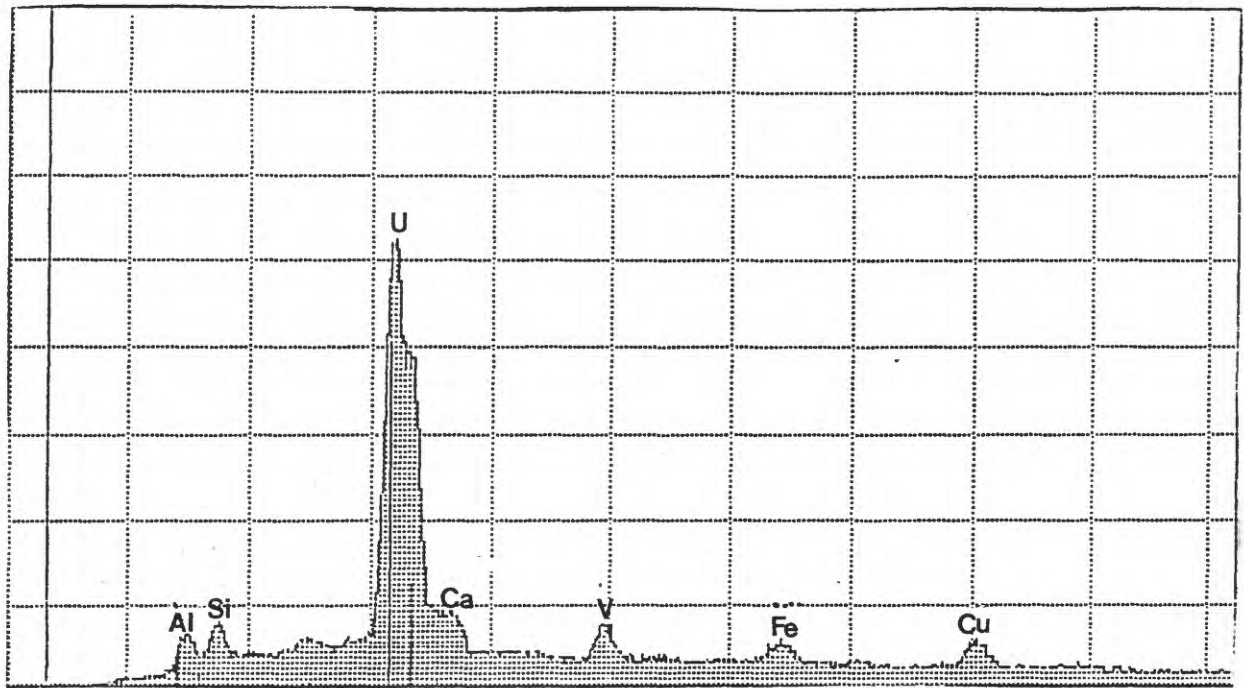
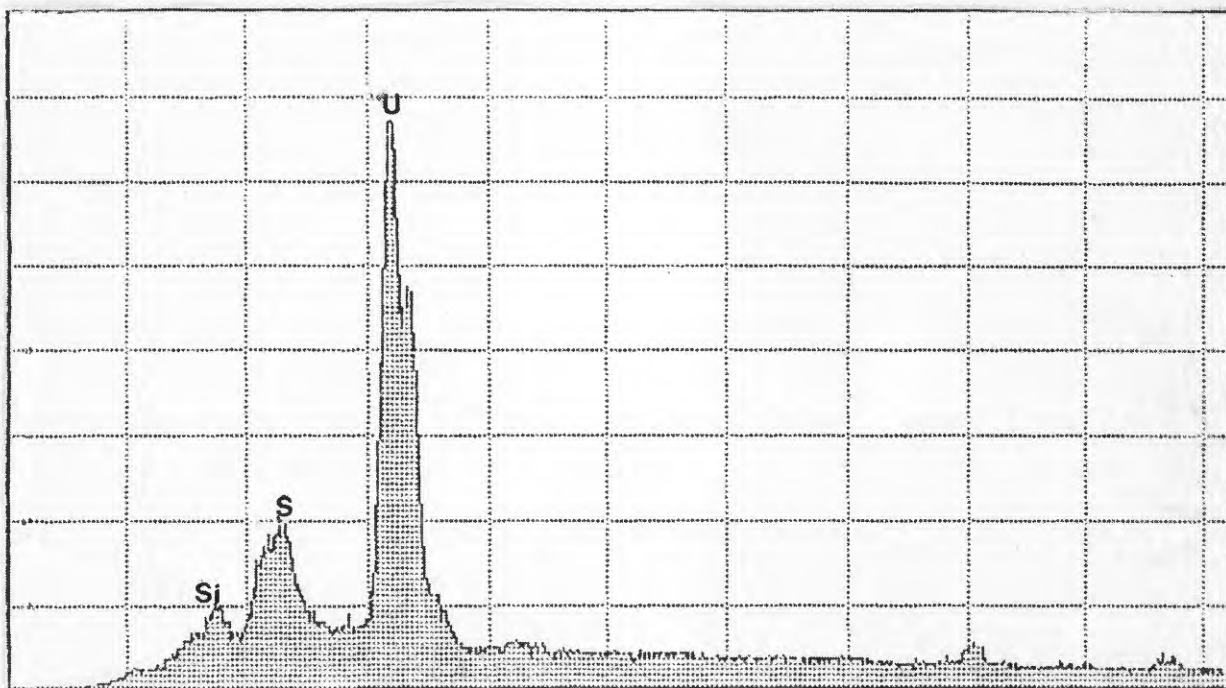


Figure 14.--SEM-EDX spectra of Al-coated polished section of ore showing an area that contains mostly U. The minor elements Si, Ca, V, and Fe show as small peaks; Cu is an artifact of the microprobe anode. Counting time, 30 seconds.



**A**



**B**

Figure 15.--(A) SEM micrograph of zippeite(?) rosettes Length of field of view is 40  $\mu\text{m}$ .  
(B) SEM-EDX spectra of Au-coated fragment that shows major U and Si; minor Si peak represents signal from an underlying quartz grain. Counting time, 30 seconds.



Figure 16.-- Photomicrograph of marcasite in polished section of ore. Length of field of view is 0.25 mm. Direct reflected light; oil immersion.

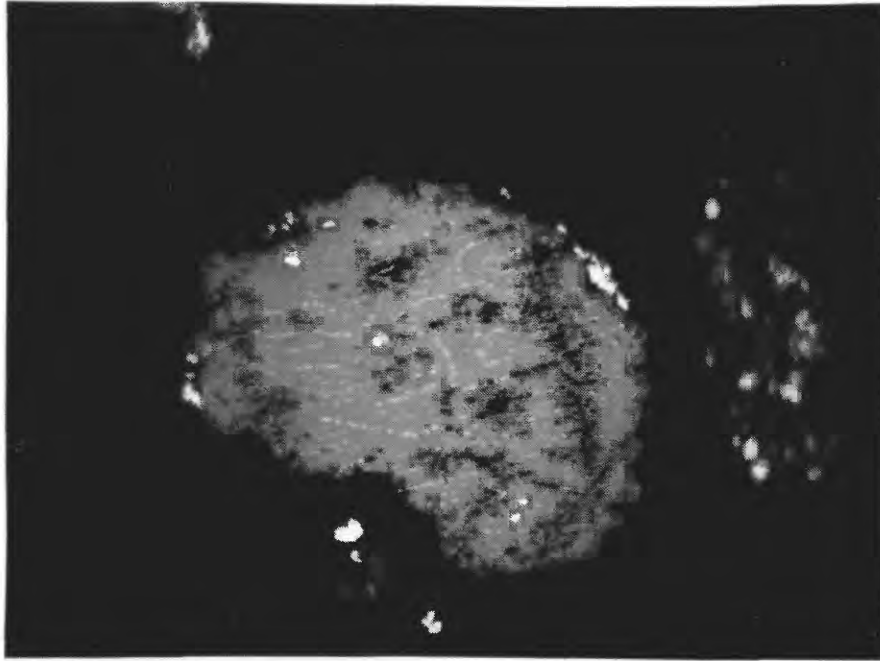


Figure 17.-- **P**hotomicrograph of polished section of uranium ore showing detrital ilmenite with hematite lamellae (aligned gray blebs). Ilmenite is generally unaltered except for minor sulfidization by pyrite (yellowish white) on the edges of the grain. Length of field of view is 0.25 mm. Direct reflected light; oil immersion.